P388.08: Microstructural variation in the human striatum using non-negative matrix factorization

Corinne Robert [1], Raihann Patel [1,3], Nadia Blostein [1,4], Christopher C. Steele [5,6], M. Mallar Chakravarty [1,2,3,7]

[1]Computational Brain Anatomy Laboratory, Cerebral Imaging Center,Douglas Mental Health University Institute, Montreal, Canada. [2]Douglas Mental Health University Institute, Verdun, Montreal, Canada. [3]Department of Biological and Biomedical Engineering, McGill University, Montreal, Canada. [4]Integrated Program in Neuroscience, McGill University, Montreal, Canada. [5]Department of Psychology, Concordia University, Montreal, Canada. [6]Department of Neurology, Max Planck Institue for Human Cognitive and Brain Sciences, Liepzig, Germany [7]Department of Psychiatry, McGill University, Montreal, Canada.

Background

The existing parcellations of the striatum have failed to characterize the tissue microstructure that necessarily constrains its organization and variation.

Goal

We aimed to integrate several neurobiological properties to capture the multiple dimensions of the striatal organization and function. More specifically, we first wanted to estimate a voxel-level data-driven microstructural parcellation using a multimodal approach. Additionally, we aimed to relate inter-individual variations in the microstructural patterns to motor and cognitive performance, age, sex, and brain function.

Methods

Data acquisition:

- 329 unrelated subject from the Human Connectome Project S1200 subject release (mean age 28.44 years ± 3.70,185 females)[1]
- Microstructure : T1- over T2-weitghted images (T1w/T2w), fractional anisotropy (FA) and mean diffusivity (MD).

Image processing: minc-bpipe library (preprocessing), MAGeT Brain algorithm[2](automatic striatal segmentation), Advanced Normalization Tools (ANTs)[3](non-linear registration).

The methods used for the microstructural and microstructure-behaviour analyses are described in figure 1.

Figure 1 A) We used vertex-wise T1w/T2w, FA and MD measures of the majority voted striatum labels to construct an input matrix **B)** We concatenated the striatal voxels in column vectors of all our subjects to build an input matrix. The left and right input matrix were build independently. **C) We extracted spatially distinct components representing patterns of covariance in microstructure across subjects using orthogonal projective non-negative matrix factorization (OPNMF)[4,5]**. OPNMF decomposes an input matrix into a component matrix W and a weight matrix H. As OPNMF extracts a predefined number of components k, we performed a stability analysis to assess the accuracy and spatial stability at each granularity from 2 to 10 [5] (see fig. 2C). **D)** (Top)The component matrix W describes how much each voxel weight into a specific component providing spatial information about the clusters. (Bottom)**We related each component to functional MRI findings by using the Neurosynth reverse-inference framework that meta-analytically relates striatal components to psychological states[7]. E)**The weight matrix H contains the weight of each subject's metrics onto each component, describing microstructural variation in the metrics found in the input matrix (T1w/T2w, FA, MD) between subjects. **F) We used Partial Least Squares (PLS) analysis to identify patterns of covariance between the striatal components T1w/T2w, FA and MD proportions with behavioural and demographic data[6].** PLS is a multivariate technique that analyses the association between our component-metric pairs (leftmost top) and selected behaviour/demographics (leftmost bottom) variables resulting in a set of latent variables (LV). The significance of the covariance patterns uncovered by the LVs was assessed using permutation testing while the reliability of each brain specific weight was assessed using bootstrap sampling.

Workflow

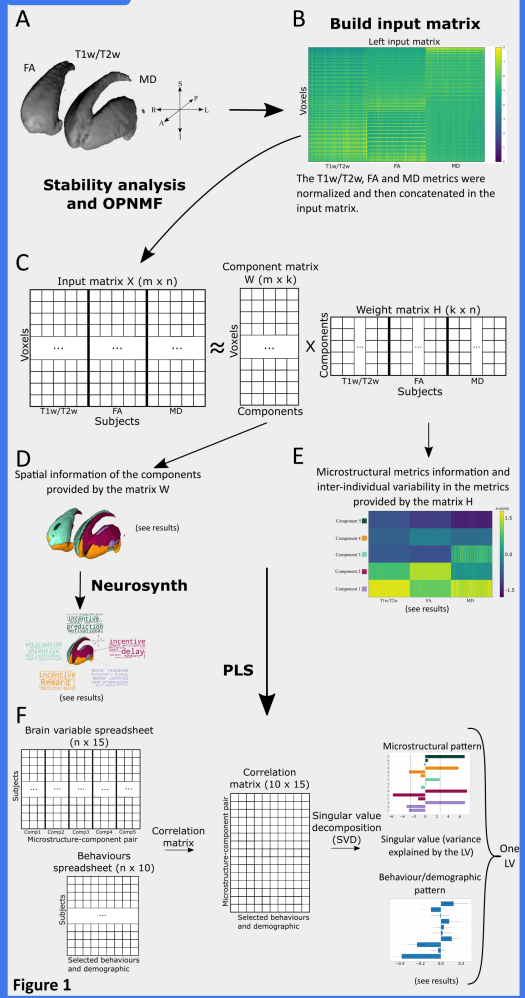

Figure 1

Results

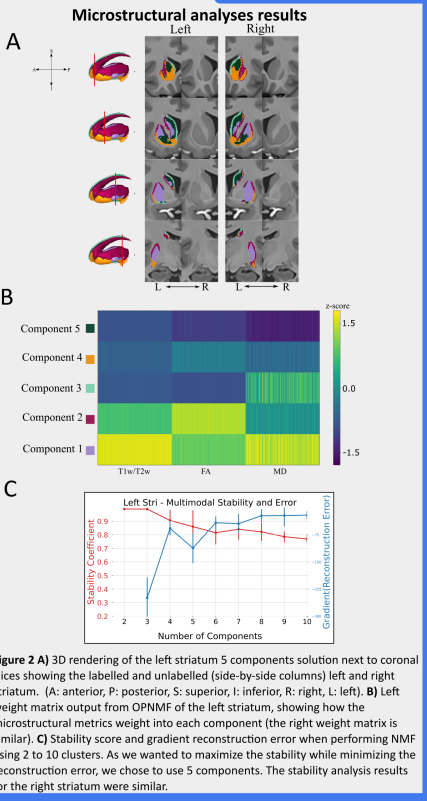

Figure 2 A) 3D rendering of the left striatum 5 components solution next to coronal slices showing the labelled and unlabelled (side-by-side columns) left and right striatum. (A: anterior, P: posterior, S: superior, I: inferior, R: right, L: left). **B)** Left weight matrix output from OPNMF of the left striatum, showing how the microstructural metrics weight into each component (the right weight matrix is similar). **C)** Stability score and gradient reconstruction error when performing NMF using 2 to 10 clusters. As we wanted to maximize the stability while minimizing the reconstruction error, we chose to use 5 components. The stability analysis results for the right striatum were similar.

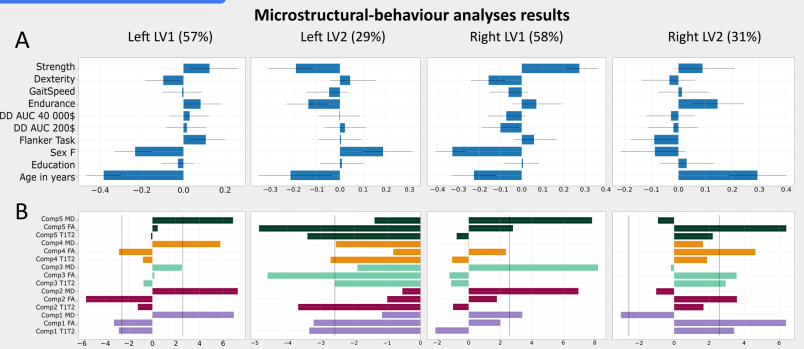

Figure 3 Results of the PLS analysis. We show only the latent variables (LVs) that were significant (p<0.05). The percentage next to the LV's name corresponds to the covariance explained by this LV. **A)** Behavioural patterns of the left LV1 (first column), left LV2 (second column), right LV1 (third column) and right LV2 (fourth column). The y-axis denotes the behavioural and demographics measures used in the analysis (DD AUC: Delay discounting area under the curve), while the x-axis corresponds to the correlation of the behaviours with the LV. **B)** Microstructural patterns associated with the four significant LVs identified. Here,the y-axis correspond to the component-metric pairs and the x-axis denotes the bootstrap ratio (BSR). The black line in the microstructural patterns graph represent a BSR of 2.58 (equivalent to a 99% C.I.). The colors of the bars are associated with the component (see figure 2B).

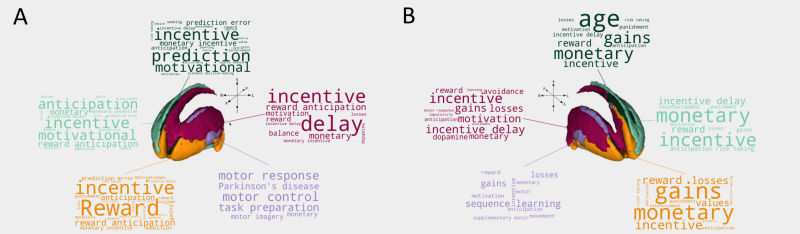

Figure 4 Left **(A)** and right **(B)** striatal components Neurosynth results. Here, the color of the words describes the component to which the posterior probability maps were related to (see figure 2B). The font of the words represents the Pearson correlation strength between the component and the keyword related map from Neurosynth. We note that the keywords' font were not normalized across components. Hence, the keyword with the biggest font represents the term with the biggest correlation in that component and not in all components.

Conclusion

- We developed a data-driven multimodal parcellation of the striatum using a combination of T1w/T2w, FA and MD images.
- We related inter-individual variations from the normative microstructural patterns to motor and cognitive performance and demographics using multivariate techniques.
- We investigated how the obtained striatal microstructural patterns related to brain function using a meta-analysis of fMRI findings.
- We identified 5 distinct striatal components by assessing the stability and accuracy of the OPNMF decomposition in a split-half stability analysis. Further we found 4 significant latent variables, 2 for each the left and right hemispheres.
- **Our analyses identified 5 spatially distinct striatal components that differ in their microstructural organisation (fig. 2). We also show that the striatal components are associated with complex patterns of microstructure and behaviour variability (fig. 3). Further, the identified components appear to be functionally relevant (fig. 4).**

References

[1]Van Essen, D.C., et al., The WU-Minn Human Connectome Project: An overview. NeuroImage, 2013. 80: p. 62-79. **[2]**Chakravarty, M.M., et al., Performing label-fusion-based segmentation using multiple automatically generated templates. Human Brain Mapping, 2013. 34(10): p. 2635-2654. **[3]**Avants, B.B., N. Tustison, and G. Song, Advanced normalization tools (ANTS). Insight j, 2009. 2(365): p. 1-35. **[4]**Sotiras, A., S.M. Resnick, and C. Davatzikos, Finding imaging patterns of structural covariance via Non-Negative Matrix Factorization. NeuroImage, 2015. 108: p. 1-16. **[5]**Patel, R., et al., Investigating microstructural variation in the human hippocampus using non-negative matrix factorization. NeuroImage, 2020. 207: p. 116348. **[6]**Zeighami, Y., et al., A clinical-anatomical signature of Parkinson's disease identified with partial least squares and magnetic resonance imaging. NeuroImage, 2019. 190: p. 69-78. **[7]**Yarkoni, T., et al., Large-scale automated synthesis of human functional neuroimaging data. Nature Methods, 2011. 8(8): p. 665-670.